Exp Brain Res (2004) 158: 180–188
DOI 10.1007/s00221-004-1892-3

RESEARCH ARTICLES

J. R. McClung · K. E. Cullen · M. S. Shall ·
D. M. Dimitrova · S. J. Goldberg

Effects of electrode penetrations into the abducens nucleus of the monkey: eye movement recordings and histopathological evaluation of the nuclei and lateral rectus muscles

Received: 8 October 2003 / Accepted: 6 January 2004 / Published online: 24 June 2004

Abstract Two adult rhesus monkeys that had undergone 2 years of electrode penetrations into their abducens and vestibular nuclei, for chronic eye movement studies, were examined histologically. An analysis of their VIth nucleus neurons and lateral rectus muscles revealed the following. Twenty-two percent of the large neurons (≈30 μm in diameter), on average, were missing and extensive neuropil disruption and gliosis was evident in the experimental side abducens nuclei as compared with the control side in each animal. While the lateral rectus muscles showed small, but inconsistent, changes in total fiber number, the muscle fiber diameters were altered, leading to a more homogenous muscle and making the typical orbital and global subdivisions of the muscle less distinct. Eye movement records from before and after the electrophysiological studies were comparable. We discuss how the complex architecture of the extraocular muscles as well as the possibility of polyneuronal innervation of single muscle fibers could explain our results.

Keywords Abducens nucleus · Lateral rectus muscle · Motoneuron · Polyneuronal innervation

J. R. McClung · D. M. Dimitrova · S. J. Goldberg (✉)
Department of Anatomy & Neurobiology, POB 980709,
Virginia Commonwealth University,
1101 E. Marshall St.,
Richmond, VA 23298, USA
e-mail: sgoldber@hsc.vcu.edu
Tel.: +1-804-8289529
Fax: +1-804-8289477

M. S. Shall
Department of Physical Therapy, Virginia Commonwealth University,
Richmond, VA 23298, USA

K. E. Cullen
Department of Physiology, McGill University,
Montreal, Quebec, H3G1Y6, Canada

Introduction

During the last quarter of a century, many of the studies that helped elucidate the neuronal control of eye movement included chronic procedures where multiple electrode penetrations were made into the extraocular muscle nuclei of alert monkeys (for reviews see Fuchs et al. 1985; Scudder et al. 2002). These investigations were carried out over extended periods of time and the neuronal recordings demonstrated normal firing patterns as well as normal and precise eye movements. It was shown, importantly, that all motoneurons (MNs) appeared to participate in all types of eye movements and those movements were precisely yoked to the firing pattern changes in each recorded MN (reviewed in Scudder et al. 2002). However, these studies may also have been important in demonstrating how the oculomotor nuclei respond to injury and neuronal cell death. These animals often had hundreds of electrode penetrations into their extraocular muscle nuclei and yet their eye movements and fixations remained normal as judged by behavioral testing.

Multiple electrode penetrations during eye movement behavioral studies likely destroy a significant number of neurons. The possibility that extraocular muscle motoneurons could be destroyed without affecting eye movements may correlate with the finding that there appears to be an overabundance of MNs in the cat and primate EOM nuclei (McClung et al. 2001; Shall et al. 2003). If one multiplies average motor unit force (twitch or tetanic) by the number of MNs in the EOM nuclei, one would expect to see a much stronger force than is actually seen when the muscle nerve is stimulated supramaximally (Goldberg et al. 1998; Shall et al. 2003). Force is lost. For example, if the average single motor unit twitch contraction force in the squirrel monkey of 10.7 mg is multiplied by the approximate number of 2,000 lateral rectus muscle motoneurons, one would expect to see a whole muscle twitch tension of 21.4 g. However, the actual average whole muscle twitch tension in response to supramaximal whole nerve stimulation is about 1.1 g (Goldberg et al. 1998; Shall et al. 2003). Such a discrepancy is not seen in

other skeletal muscle (Burke et al. 1973; Kernell et al. 1985).

Another factor that could play a role in preserving normal eye movements with the possible loss of final common path motoneurons is polyneuronal innervation of single muscle fibers. Although an early physiological study indicated that polyneuronal innervation was not evident in the VIth nerve innervated lateral rectus muscle of the adult cat (Bach-y-Rita and Lennerstrand 1975), we and others have suggested that the multiply innervated fibers of adult EOMs may be innervated by more than one neuron (Muhlendyck 1978; Jacoby et al. 1989; McClung et al. 2001). It has long been known that young animals exhibit polyneuronal innervation (Brown and Matthews 1960) while developmental myosin heavy chain (MHC) isoforms are expressed. Neither polyneuronal innervation nor developmental MHC isoforms are prevalent in adult animals. However, it is notable that the EOMs are an exception in that developmental MHC isoforms are expressed throughout an animal's lifetime (Wieczorek et al. 1985; Jacoby et al. 1989; McLoon et al. 1999). Polyneuronal innervation, then, may also play a role in the apparent loss of force seen in extraocular muscle, as well as helping to preserve normal eye movements while MNs are lost.

We have, therefore, undertaken a thorough histological evaluation of the abducens nuclei and the lateral rectus muscles from two monkeys that were subjects in chronic neurophysiological studies of their eye movements for more than 2 years (Sylvestre and Cullen 1999). The examples of eye position and velocity profiles of different size saccades (3–30°) recorded late in the cited study look quite normal (Sylvestre and Cullen 1999). Problems in gaze holding during fixation or decreases in peak velocity of the saccades might be expected following substantial neuron loss in the abducens nucleus. That these chronic neurophysiological recordings would cause some destruction is a given, but the extent of that damage needs to be documented since the eye movements remained remarkably unimpaired. To our knowledge, a detailed histological examination of such animals has not been done previously.

Materials and methods

Two adult Rhesus monkeys that had been subjects in chronic, electrophysiological recording studies were examined histologically. Animal 1 was 7 years old when the physiological experiments started (born November 1990) and Animal 2 was 10 years old (born August 1988). All eye movement recordings shown are from Animal 1. Recording from the abducens nuclei were done over a period of 1 year and vestibular recording were made during the following year. The animals were sacrificed for histological study at the end of the second year.

Eye movement recordings

All procedures were approved by the McGill University Animal Care Committee and were in compliance with the guidelines of the Canadian Council on Animal Care. The methods for surgical preparation of the monkeys were similar to those described by Sylvestre and Cullen (1999). Briefly, under general anesthesia and aseptic conditions, a scleral search coil was implanted in each monkey in order to monitor gaze position, and a stainless-steel bolt was attached to the skull for restraining the head. During each experiment, a monkey was comfortably seated in a stationary primate chair that was placed in the center of a 1-m^3 magnetic field coil system (CNC Engineering). Eye position was recorded with the magnetic search coil technique (Fuchs and Robinson 1966; Judge et al. 1980). Monkeys were trained to track a small (0.3 deg in diameter) visual target for a juice reward. Target motion was generated using a HeNe laser spot that was projected on a white cylindrical screen, located 60 cm away from the monkey's eyes, by a pair of mirrors mounted on two computer-controlled galvanometers (General Scanning). REX, a QNX-based real-time data acquisition system (Hayes et al. 1982), was used to control target position, monitor performance, and to collect data. Eye and target position signals were filtered (eight-pole Bessel, DC-250 Hz) and then digitized at 1 KHz.

Animal 1 had 59 electrode penetrations in the left abducens nucleus, ten in the right abducens nucleus (control) and 200 in the left vestibular nucleus. Animal 2 had 100 abducens nucleus penetrations on the left and 20 on the right (control) plus 40 others, mainly in the left vestibular nucleus. At the conclusion of the experiments the animals were overdosed with sodium pentobarbital and killed by transcardiac perfusion with 10% neutral buffered formalin. The brain and orbital contents were carefully removed and photographed before the brain stem and lateral rectus muscles were embedded in paraffin. Ten-micrometer, serial, transverse sections were made through the pons at the level of the VIth and VIIth cranial nerve nuclei as well as through the central region of the lateral rectus muscles from both orbits.

Muscle histology

Each muscle was bisected at its mid-belly (≈1.5 cm proximal to the tendon insertion) and was embedded in paraffin wax using a traditional 'carousel' type automatic processor (Shandon-Lipshaw Citadel 2000) using a 12-h schedule. Each muscle was oriented in plastic and metal molds for transverse sectioning. Ten micron sections were cut using a microtome and mounted on standard coated microscope slides. The slides were then processed with a standard hematoxylin and eosin stain. After staining, the slides were dehydrated in alcohol and cleared with xylene and cover slipped with resin.

A magnified video image of a single representative section from each muscle's mid-belly was sent to a PC for analysis of muscle fiber total number and size. Samples of clearly identifiable orbital (3,000) and global (5,000) muscle fibers from each animal's experimental and control side muscles were used for measurements of fiber minimum mean diameter. Measurements were made using an image analysis software package (Media Cybernetics Image-Pro Plus version 4.5). The experimental side was compared with the control side using the unpaired *t*-test.

Histological analysis of the abducens nuclei

Alternate sections of the pons demonstrating the right and left abducens nuclei were stained with Klüver and Barrera (luxol fast blue/cresyl violet) or GFAP stains. The Klüver and Barrera stain shows nerve fibers (blue) and neuron cell bodies (violet). The GFAP (glial fibrillary acid protein) reaction using the SMI 21 monoclonal antibody (Sternberger Monoclonals Inc., Lutherville, MD, USA) stains astrocytes and their processes brown.

Motoneuron distribution in the abducens nucleus is shown here (Fig. 2a) using retrograde transport of HRP (McClung et al. 2001) from the lateral rectus muscle. This section is from a Rhesus monkey not used in any physiological study and is shown in Methods to demonstrate a normal nucleus and MN location. These

lateral rectus muscle (LR) MNs are seen to be a homogenous population of large (30 μm) cells found within the arch of the facial nerve genu as described for the abducens nucleus of the squirrel monkey (McClung et al. 2001). A MN diameter of 30 μm also appears to represent large cells (according to a histogram) in the monkey abducens nucleus (Büttner-Ennever et al. 2001). Therefore, in the present study we counted similar sized (30 μm) neurons (containing substantial Nissl substance) observed within a 1.0-mm^3 field taken from the center of the abducens nucleus near the genu of the VIIth nerve. Since the abducens nucleus contains two subpopulations of neurons—motoneurons that project to the ipsilateral lateral rectus and internuclear neurons that project to medial rectus motoneurons (OMNs) in the contralateral oculomotor nucleus (Delgado-Garcia et al. 1986a, b), we use "neurons," rather than "motoneurons" throughout the paper. Nucleoli of these neurons were counted in single sections showing both control and experimental sides. The sections used were spaced at least 50 μm apart to eliminate any double counting of the same cell (Fig. 2b). Total cell counts and individual section counts from the experimental and control sides were tabulated and statistically compared using the Mann-Whitney test.

Results

Eye movement records

Figure 1 demonstrates typical, neurophysiological records of eye position (Ep) and velocity (Ev) taken during eye movements in Animal 1. Figure 1a shows recordings taken at the beginning of the study before any electrode penetrations. Figure 1b shows recordings from the same animal after 59 electrode penetrations into the VIth nucleus had been done. Figure 1c demonstrates some small readjustments taking place during eye fixation, fixation drift and some minor position shifts (leftward correction saccades) occurring during pursuit eye movement. These minor changes in eye movement are following an additional year of electrode penetration studies including some 200 recordings from the vestibular nuclei, just lateral and caudal to the abducens nucleus.

In each animal, the velocity and accuracy of visually guided saccades and gain of smooth pursuit eye movements were not altered following single unit recording experiments in the abducens nucleus. A common feature of eye movements in primates (Bahill et al. 1975; Fuchs et al. 1985) is the relatively fixed relationship that exists between saccade amplitude and peak velocity. This relationship is called the main sequence. A linear regression on the main sequence relationship for saccades (amplitude range: 3–30 deg) directed towards the side of the recordings revealed slopes of 15.1 versus 16.1 deg/s per deg, and 16.4 versus 16.2 deg/s per deg, for Animals 1 and 2, respectively. Differences in slopes were not statistically significant for either animal ($p>0.05$; note, a linear regression rather than an exponential fit was used to fit the data because the main sequence relationship was well approximated as a straight line in both animals [R values >0.7]). In addition, electrode penetrations into the abducens nucleus did not have a consistent effect on saccade amplitude in either animal, indicating that saccade accuracy was not affected. Moreover, smooth pursuit gain

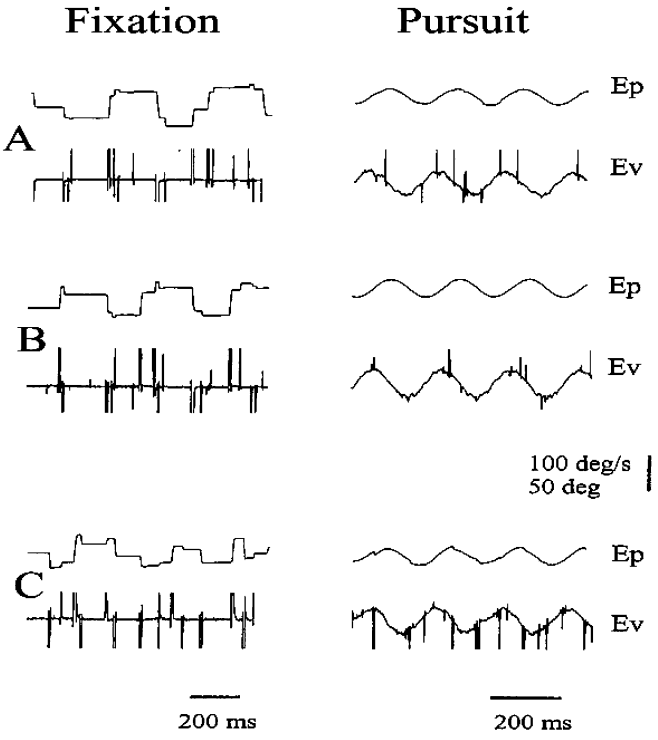

Fig. 1a–c Physiological recordings of eye movement from Animal 1. Horizontal eye movement position (*Ep*) and velocity (*Ev*) during saccades and Fixation (labeled) plus Pursuit (labeled) are shown. Downward deflections represent movements to the left. **a** Normal eye movements (before any electrode tracks). **b** After all of the abducens nucleus electrode penetrations had been done during a period of 1 year (unchanged from the normal). **c** Following study of the adjacent vestibular nucleus (200 electrode penetrations) during the next year. A slight eye drift is noted in the fixation record and small corrections are seen during pursuit

remained comparable in Animal 2, while it actually increased in Animal 1 (0.87 to 0.98). This increase in gain, most likely reflected that the additional training received during electrophysiological studies served to improve Animal 1's performance. Finally, Animals 1 and 2 were generally able to maintain stabile fixation following the abducens recordings. The only consistent effect of the electrode penetrations into the abducens nucleus was observed in Animal 2. In this animal, a small (<10 deg/s) drift in eye position was observed after saccades, which brought the eye 15 deg or more to the left of center position.

Abducens nucleus

Luxol fast blue staining of nerve fibers (myelinated axons) (Fig. 2b–d) shows a substantially different neuropil in the experimental nucleus when compared with that of the control abducens nucleus. The experimental side demonstrates several electrode tracks (*arrows* in Fig. 2b). This nucleus is nearly devoid of large myelinated fiber bundles (Fig. 2b, d) as compared with the control side (Fig. 2c). Even the genu (g) of the seventh nerve shows a substantial decrease in fiber staining as a result of electrode track

damage (Fig. 2b). Cresyl violet (Nissl) staining of the neurons is shown in these same sections. While few neurons are seen within the electrode tracks, normal looking neurons are observed in other areas of the experimental nucleus (Fig. 2d). Neuron counts showed an average 22% reduction in neuron number on the experimental side as compared with the control side (Table 1). It is also interesting to note that the monkey that had 59 direct penetrations into the abducens nucleus (Animal 1) showed an 18.5% reduction in neuron number while Animal 2, which had 100 direct penetrations into the abducens nucleus, showed a 25.2% reduction in neuron number. Additionally, Animal 1 had 200 penetrations into the surrounding vestibular nuclei and Animal 2 had only 60 other penetrations. The genu of the facial nerve can also be observed and was found to be lacking fiber staining as a result of the electrode penetrations (*right side* of Fig. 2b). Due to this facial nerve damage, we also looked at the facial nucleus and the muscles of facial expression in Animal 1 and found them to be reduced in size upon visual examination and comparisons to the control side. However, no quantification was attempted since this was outside of the scope of this study and we had no physiological records on the activity of the facial muscles.

GFAP staining of astrocyte cell bodies and processes (Fig. 2e, f) demonstrate that astrocytes are filling the void produced by the loss of neuron cell bodies and nerve fibers within the abducens nucleus. GFAP reaction (brown

Table 1 Comparison of the number of neurons between sides and between animals

Abducens nucleus	Animal 1*		Animal 2**	
	Control	Experimental	Control	Experimental
Total number	367	299	404	302
Range per section	28–51	25–38	21–51	21–35
Percentage loss	-	18.5% loss	-	25.2% loss

*Animal 1: experimental is significantly different from control ($p<0.05$)
**Animal 2: experimental is significantly different from control ($p<0.01$)

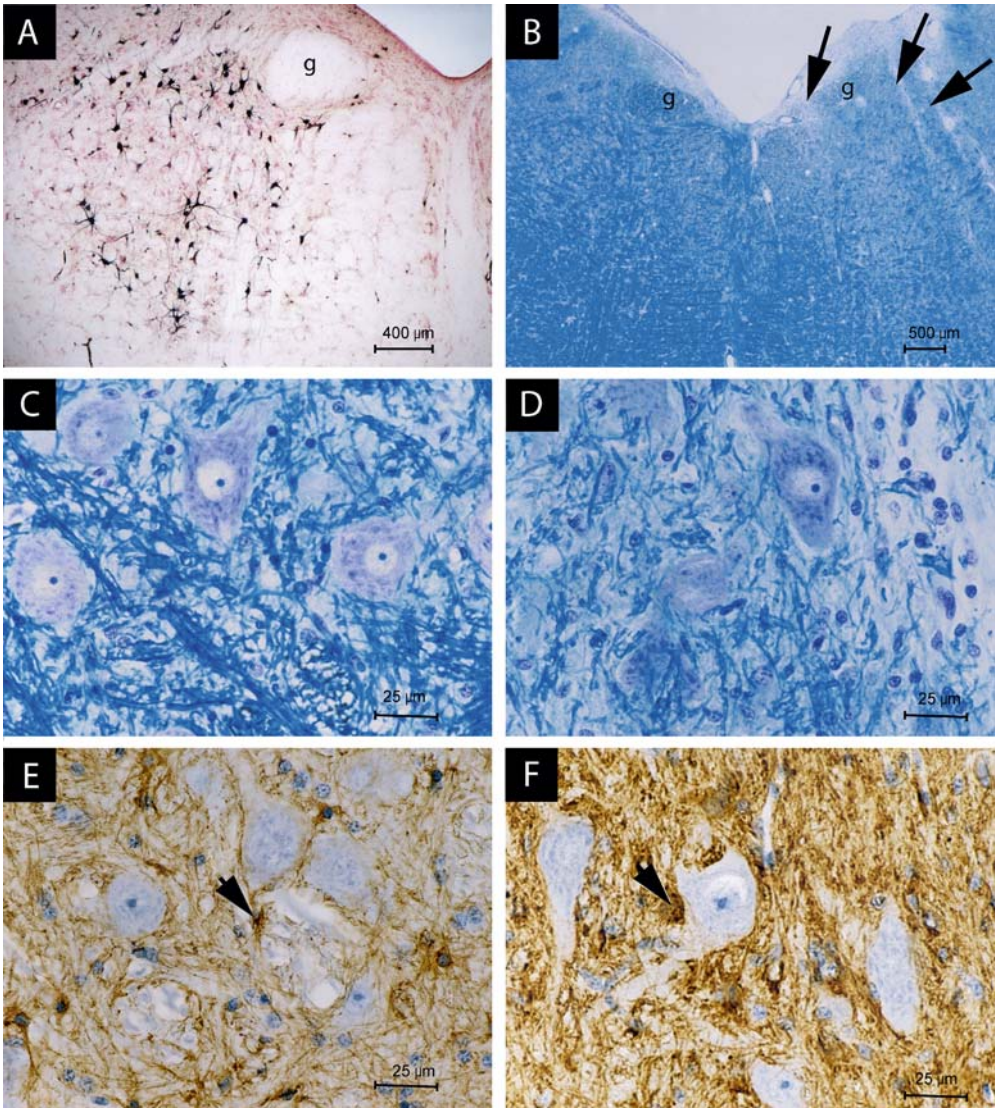

Fig. 2a–f Histology of the abducens nucleus. **a** Retrograde labeling (HRP) from the lateral rectus muscle of a normal Rhesus monkey. Lateral rectus muscle motoneurons are labeled in the center of the abducens nucleus, arched over by the VIIth nerve genu (*g*). **b** A midline section showing both the right and left sides of the abducens nucleus. The nucleus on the *left side* of the figure is the control and the experimental side is on the *right side* of the figure. Note electrode tracks at *arrows.* **c** High magnification view taken from the control side of section (**b**, *left*) showing large multipolar neurons (≈30.0 µm diameter). Note the heavily stained bundles of nerve fibers in the neuropil. (Klüver-Barrera stain). **d** High magnification view taken from the experimental side of section (**b**, *right*) showing some normal multipolar neurons. Note the lack of bundles of nerve fibers in the neuropil. (Klüver-Barrera stain). **e** A view of the control side (similar to **c** above) with GFAP reaction showing the astroglia (*brown*). Note the small, filamentous nature of the astrocyte cell bodies (*arrow*). **f** A view of the experimental side (similar to **d** above) with GFAP reaction (*brown staining*) showing the reactive protoplasmic astrocytes and extensive gliosis in the neuropil

staining) is significantly increased on the experimental side (Fig. 2f) as compared with the control side (Fig. 2e). The astrocyte cell bodies are also larger and more protoplasmic in the experimental nucleus (Fig. 2f, *arrow*) as compared to those on the control side (Fig. 2e, *arrow*).

Lateral rectus muscle

Lateral rectus muscles from both sides (control in the *left panels* of Fig. 3 and experimental in the *right panels* of Fig. 3) were found to have a classical, extraocular muscle configuration consisting of a global and orbital layer (Spencer and Porter 1988). The orbital layer (small fiber diameter cap) is observed on the external surface (near the orbital wall) and a global layer of larger muscle fibers in seen internally (toward the eyeball) (Fig. 3a, b). A transitional zone or intermediate layer separates the two distinctive layers. The total number of muscle fibers counted in a single section taken from the mid-belly of each animal's lateral rectus muscles is as follows. Animal 1 had 9,011 fibers on the experimental side and 10,068 on the control side. Animal 2 had 11,622 fibers on the experimental side and 9,066 on the control side.

Higher magnification views (Fig. 3c–f) demonstrate the change in fiber size observed in the orbital and global layers of the lateral rectus muscle when the experimental side (Fig. 3b, d, f) is compared with the control side (Fig. 3a, c, e). The distinctively smaller diameter of the muscle fibers in the control orbital layer as compared with the control global layer is obvious. This is shown numerically in Table 2 and by the clearly bimodal fiber size distribution in the histogram of Fig. 4a. Comparison of the muscles from the experimental side to the control side demonstrates a reorganization of the lateral rectus muscle following injury to its motoneurons in the abducens nucleus (Fig. 3 and Table 2). On the experimental side the muscle showed a tendency to become more homogenous in fiber diameter following injury to its innervating motoneurons. The orbital muscle fibers are larger or unchanged on the experimental side while the global fibers are smaller when compared with the control side (Fig. 3). Quantification of these muscle fiber size changes is delineated in Table 2 and illustrated graphically in Fig. 4b. Even though the amount of change varies, the tendency toward muscle fiber size homogeneity is supported in both animals. The muscle on the experimental side of Animal 1 (59 VIth nucleus penetrations) showed a 40% increase in the diameter of the small orbital

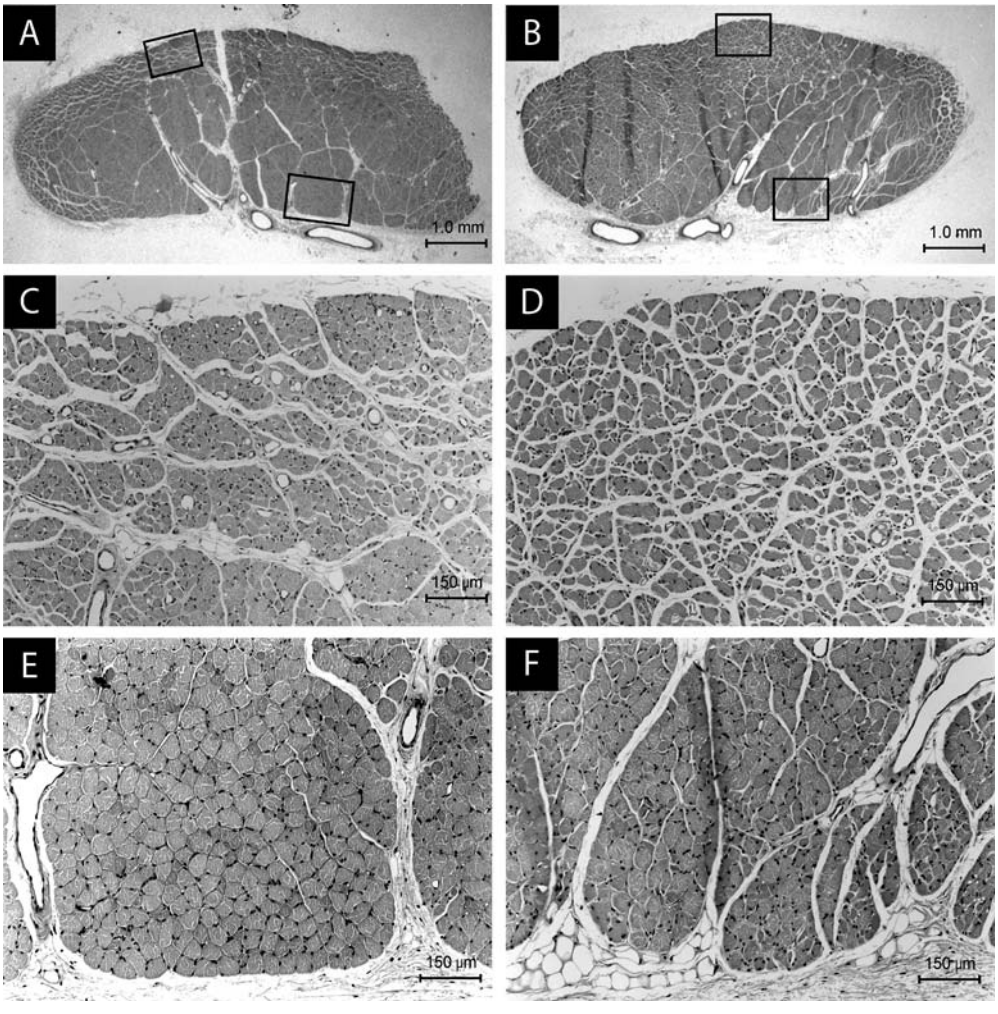

Fig. 3a–f H & E histology of the lateral rectus muscle of Animal 2. **a, c** and **e** (*left-side panels*) are from the LR muscle from the control side. **b, d** and **f** (*right-side panels*) are from the experimental side where electrode penetrations were made into the abducens nucleus. **a** and **b** Low-magnification views. Note the small fibers of the orbital layer near the top of each figure (*rectangle*) and the larger fibers of global layer, near the bottom of each figure. The areas of the rectangles are magnified in **c** and **d** (orbital layer) and **e** and **f** (global layer) for each muscle. Note increased fiber diameters in the orbital layer and decreased fiber diameters in the global layers of the muscle from the experimental (*right*) side as compared with the control

muscle fibers, while the larger global muscle fibers decreased in diameter by 37% as compared with the control side. In Animal 2 the orbital fibers on the experimental side (100 abducens penetrations) remained relatively unchanged while the global fibers showed a substantial 25% decrease in average muscle fiber diameter as compared with the control side (20 VIth nucleus penetrations).

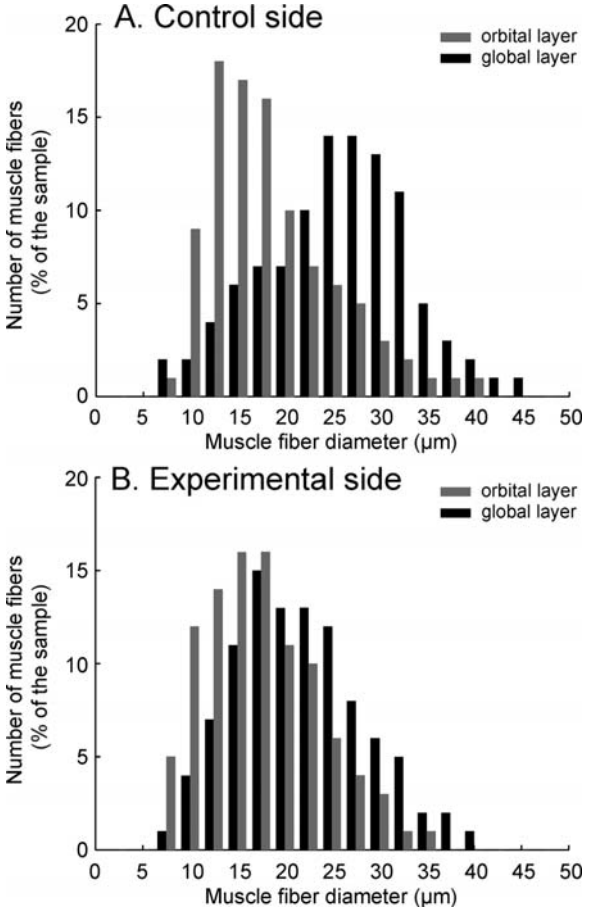

Fig. 4a, b Distribution of muscle fiber diameters in the orbital and global layers of the lateral rectus muscle of Animal 2. **a** Control side and **b** experimental side

Discussion

Major changes were observed in the neuropil of the abducens nuclei of two monkeys following repeated electrode penetrations for study of their eye movements during the last 2 years of their lives. Neuron number decreased by an average of 22% in the abducens nuclei on the experimental side. Myelinated axon profiles were greatly reduced, while astrocytic profiles increased and astrocyte cell bodies appeared larger and more protoplasmic in the injured nucleus as compared with the control side.

Significant differences in muscle fiber diameter were seen in the lateral rectus muscle from the experimental side of these monkeys as compared with the control side. While the number of muscle fibers differed between the lateral rectus muscle on the experimental side versus the control side, we found this difference to be inconsistent. But the total number of muscle fibers observed (≈10,000 for each lateral rectus muscle) is similar to that reported previously for the Rhesus monkey (Peachey 1971). However, changes in muscle fiber diameter on the experimental side altered the normal architecture of the muscle. The orbital layer of the lateral rectus muscle, which normally contains smaller diameter muscle fibers, remained unchanged or showed an increase in average muscle fiber diameter on the experimental side. The global layer, which is made up of predominately larger muscle fibers, consistently showed a decrease in muscle fiber diameter following disruption of its motor nucleus. These muscle fiber size changes resulted in the lateral rectus muscle becoming more homogeneous. That is, the orbital and global layer subdivisions became less definitive regarding fiber diameter.

The neurophysiological records showed only minor changes in the monkeys' ability to make eye movements following 59 to 100 electrode penetrations into the

Table 2 Comparison of the lateral rectus muscle fiber least diameter by layer and side

Layer of muscle	Animal 1		Animal 2	
	Control	Experimental	Control	Experimental
Orbital layer				
Mean (μm)	16.25±0.08*	22.79±0.13*†	16.82±0.12*	16.16±0.11*†
Range (μm)	7.13–31.92	7.43–54.62	3.66–51.47	4.07–44.62
Global layer				
Mean (μm)	30.44±0.16	19.26±0.1†	24.35±0.15	20.32±0.09†
Range (μm)	10.63–67.27	1.23–45.7	3.66–60.52	1.91–52.04

* Orbital vs. global layer muscle fiber diameter. On the control sides of both animals, the least diameters of the orbital layer muscle fibers were significantly smaller than the global layer muscle fibers ($p<0.001$). On the experimental side, the orbital muscle fibers were also smaller than the global muscle fibers in Animal 2 but not in Animal 1

†Experimental vs. control side muscle fiber diameter. The orbital layer muscle fiber diameters are significantly larger on the experimental side (compared with the control side) of Animal 1 but not Animal 2. The global layer muscle fiber diameters are significantly smaller ($p<0.001$) on the experimental side in both animals

abducens nucleus. This is somewhat unexpected since all abducens neurons have been found to participate in horizontal eye movement.

The organization, but not the number, of the muscle fibers in the lateral rectus muscles changed following injury to the abducens nucleus. Eye movements, however, remained remarkably unimpaired. This might indicate that some amount of axon branching and muscle fiber re-innervation had taken place. Commonly, after nerve injury, neuromuscular junctions are re-innervated by the remaining uninjured neurons, resulting in larger motor units (Waldeck et al. 1995). Consequently, these new larger motor units might be expected to be less precise, but no obvious oculomotor deficit was apparent. It has also been suggested that the cerebellum (specifically the vermis, paravermis, and fastigial nuclei) can compensate for a peripheral muscle weakness induced by tenectomy of both the lateral and medial recti muscles (although muscle force was not measured) (Optican and Robinson 1980). Recently, some changes in the discharge pattern of fastigial nucleus neurons were found to correlate with saccade size adaptation following muscle weakening (Scudder and McGee 2003). Indeed, these findings are consistent with the present study. Here the neuromuscular system could compensate for the effect of multiple electrode penetrations into the abducens nucleus. While it is possible that the compensation was mediated in part by the drive from the cerebellum, it is also possible that mechanisms at the level of the muscle were involved.

Such mechanisms at the level of the muscle could include polyneuronal innervation of single muscle fibers as well as the complex architecture known to exist in EOMs (Mayr et al. 1975; Shall et al. 2003) and other skeletal muscles (Monti et al. 2001). The orbital and global layers of the extraocular muscles in mammals (including primates and man) have been shown to contain single muscle fibers with multiple neuromuscular junctions. Such multiply innervated muscle fibers appear to make up 30% of the fiber population of the cat inferior oblique muscle (Alvarado and Van Horn 1975), but all of that population is certainly not comprised of nontwitch motor units (Lennerstrand 1974). That is, multiply innervated units can show twitch contractions (Lennerstrand 1974). Indeed, only 5% of cat superior oblique motor units were seen to be nontwitch units (Nelson et al. 1986). Other studies have revealed that 5–10% of cat lateral and medial rectus muscle motor units can be classified as nontwitch (Goldberg et al. 1981; Meredith and Goldberg 1986; Shall and Goldberg 1992, 1995) and these nontwitch units appeared confined to the muscle's global layer (Shall and Goldberg 1995). It has also been documented that lateral rectus muscle nontwitch motor units are innervated by antidromically identified MNs found well within the confines of the cat abducens nucleus (Goldberg et al. 1981; Shall and Goldberg 1992, 1995) and those MNs can be quite large (40 μm in diameter) (Goldberg 1990). In contrast, a purely anatomical study has suggested that small neurons in the periphery of the EOM nuclei of primates might innervate nontwitch motor units (Büttner-Ennever et al. 2001). Interestingly, no nontwitch units were encountered (among 58 units examined) in a physiological study of the squirrel monkey abducens nucleus and lateral rectus muscle (Goldberg et al. 1998).

We and others have proposed that multiply innervated fibers may be innervated by more than one neuron (polyneuronal innervation) (Jacoby et al. 1989; McClung et al. 2001). The fibers in most skeletal muscles transition to innervation by a single MN as neuromuscular junctions are eliminated during postnatal development. Developmental MHC isoforms are replaced by slow or fast MHC isoforms which are then expressed in the adult animal (McLoon et al. 1999). The extraocular muscles are an exception in that developmental MHC isoforms are expressed throughout an animal's lifetime (McLoon et al. 1999). It would then be reasonable to propose that a significant number of lateral rectus muscle MNs could be lost before a functional reduction in the innervation of the muscle fibers would take place. Total loss of innervation would not occur for many muscle fibers, since the polyneuronally innervated fibers might still receive nerve supply from at least one MN. Applying this injury model, the lateral rectus muscle would then remain functionally normal following the loss of MNs. However, the muscle fibers would be expected to show some anatomical changes.

It also has been previously established that EOM fibers do not always run in parallel for the length of the muscle. There are serial as well as side-to-side attachments plus fiber branching (Mayr et al. 1975; Shall et al. 2003). This complex architecture implies that motor unit force would not always sum in a linear manner and we have shown that for both the cat and primate lateral rectus muscle (Goldberg et al. 1997; Shall et al. 2003). When EOM motor units are activated simultaneously their combined force output is much less than would be expected by simple addition of their individual forces.

The combination of a complex muscle architecture and polyneuronal innervation could serve to protect eye movement control from a loss of MNs and/or muscle fibers. Clearly, all the MNs are not needed for precise eye movements and fixation, since we conservatively estimate that a quarter of abducens nucleus neurons were lost during these physiological studies. A recent study showed that 44% of facial MN axons in the mouse could be lost (following peripheral nerve crush which is known not to cause neuronal cell death) before gross functional changes were evident (Kobayashi et al. 2002). It is important to note, however, that the observational assessment of whisker movement and eye blink (Kobayashi et al. 2002) was much less precise than that provided by the eye movement recordings in the primate. While the general finding of functional integrity in the face of peripheral MN loss is similar to what we report here, those authors do not comment on the possible mechanisms of their findings. In addition, the myelinated fibers normally associated with an intact VIth nucleus were notably reduced in the monkeys examined in this study.

It is tempting to hypothesize that the "extra" MNs needed to effect polyneuronal innervation plus the complex muscle architecture may be one of the ways that mammalian eye movements are protected from the effects of slow onset motoneuron damage. This theory is particularly intriguing when one looks at the number of motoneuron diseases that do not affect eye movement accuracy. Reviews of the differential susceptibility of the ocular motor system to disease list amyotrophic lateral sclerosis (ALS), poliomyelitis, progressive bulbar palsy and progressive spinal atrophy as examples of diseases which spare the MNs of the eye movement system (Gizzi et al. 1992; Kaminski et al. 2002). However, Kaminski et al. (2002) state that even though routine clinical examinations fail to identify eye movement disturbances, histopathological studies do show ocular motoneuron degeneration in a few cases of ALS and some patients show inclusion bodies that are characteristic of ALS. It may now be time to see, using postmortem histopathology, if these motoneuron diseases do reduce the number of EOM MNs even though eye movements did not appear to be impaired. Our present data indicate that a significant number of motoneurons could be affected before eye movement accuracy would be compromised. Similar data in relation to other motor systems might provide evidence as to whether the functional compensation for abducens motoneuron loss is unique or shares common mechanisms with other systems.

Acknowledgements Supported by National Institutes of Health grants EY 11249 and EY 02191 and by a Medical Research Council of Canada (MRC) grant to Dr. Cullen. The authors greatly appreciate the help of Dr. John T. Povlishock for his advice on histopathological techniques as well as the technical assistance of Sue Walker and Barbara Mann.

References

Alvarado JA, Van Horn C (1975) Muscle cell types of the cat inferior oblique. In: Lennerstrand G, Bach-y-Rita P (eds) Basic mechanisms of ocular motility and their clinical implications. Pergamon Press, Oxford, pp 15–43

Bach-y-Rita P, Lennerstrand G (1975) Absence of polyneuronal innervation in cat extraocular muscles. J Physiol 244:613–624

Bahill AT, Clark MR, Stark L (1975) The main sequence: a tool for studying human eye movements. Math Biosci 24:191–204

Brown MC, Matthews PBC (1960) An investigation into the possible existence of polyneuronal innervation of individual skeletal muscle fibers in certain hind-limb muscles of the cat. J Physiol 151:436–456

Burke RE, Levine DN, Tsairis P, Zajac FE (1973) Physiological types and histochemical profiles in motor units of the cat gastrocnius. J Physiol 234:723–748

Büttner-Ennever JA, Horn AKE, Scherberger H, D'Ascanio P (2001) Motoneurons of twitch and nontwitch extraocular muscle fibers in the abducens, trochlear, and oculomotor nuclei of monkeys. J Comp Neurol 438:318–335

Delgado-Garcia JM, Del Pozo F, Baker R (1986a) Behavior of neurons in the abducens nucleus of the alert cat. I. Motoneurons. Neuroscience 17:929–952

Delgado-Garcia JM, Del Pozo F, Baker R (1986b) Behavior of neurons in the abducens nucleus of the alert cat. II. Internuclear neurons. Neuroscience 17:953–973

Fuchs AF, Robinson DA (1966) A method for measuring horizontal and vertical eye movement chronically in the monkey. J Appl Physiol 21:1068–1071

Fuchs AF, Kaneko CRS, Scudder CA (1985) Brainstem control of saccadic eye movements. Ann Rev Neurosci 8:307–337

Gizzi M, DiRocco A, Sivak M, Cohen B (1992) Ocular motor function in motor neuron disease. Neurol 42:1037–1046

Goldberg SJ (1990) Mechanical properties of extraocular motor units. In: Binder MD, Mendell LM (eds) The segmental motor system. Oxford University Press, Oxford pp 222–238

Goldberg SJ, Clamann HP, McClung JR (1981) Relation between motoneuron position and lateral rectus motor unit contraction speed: an intracellular study in the cat abducens nucleus. Neurosci Lett 23:49–54

Goldberg SJ, Wilson KE, Shall MS (1997) Summation of extraocular motor unit tensions in the lateral rectus muscle of the cat. Muscle Nerve 20:1229–1235

Goldberg SJ, Meredith MA, Shall MS (1998) Extraocular motor unit and whole-muscle responses in the lateral rectus muscle of the squirrel monkey. J Neurosci 18:10629–10639

Jacoby J, Chiarandini DJ, Stefani E (1989) Electrical properties and innervation of fibers in the orbital layer of rat extraocular muscles. J Neurophysiol 61:116–125

Hayes AV, Richmond BJ, Optican LM (1982) A UNIX-based multiple process system for real-time data acquisition and control. WESCON Conf Proc 2:1–10

Judge SJ, Richmond BJ, Chu FC (1980) Implantation of magnetic search coils for measurement of eye position: an improved method. Vision Res 20:535–538

Kaminski HJ, Richmonds CR, Kusner LL, Mitsumoto H (2002) Differential susceptibility of the ocular motor system to disease. Ann NY Acad Sci 956:42–54

Kernell EL, Verhey BA, Eerbeck O (1985) Neuronal and muscle unit properties at different rostro-caudal levels of cat's motoneurone pool. Brain Res 335:71–79

Kobayashi S, Koyama J, Yokouchi K, Fukushima N, Oikawa S, Morizumi T (2002) Functionally essential neuronal populations of the facial motor nucleus. Neurosci Res 45:357–361

Lennerstrand G (1974) Electrical activity and isometric tension in motor units of the cat's inferior oblique muscle. Acta Physiol Scand 91:458–474

Mayr R, Gottschall J, Gruber H, Neuhuber W (1975) Internal structure of cat extraocular muscle. Anat Embryol 148:25–34

McClung JR, Shall MS, Goldberg SJ (2001) Motoneurons of the lateral and medial rectus extraocular muscles in squirrel monkey and cat. Cells Tissues Organs 168:220–227

McLoon LK, Rios L, Wirtshaffer JD (1999) Complex three-dimensional patterns of myosin isoform expression: differences between and within specific extraocular muscles. J Muscle Res Cell Motil 20:771–783

Meredith MA, Goldberg SJ (1986) Contractile differences between muscle units in the medial rectus and lateral rectus muscles in the cat. J Neurophysiol 56:50–62

Monti RJ, Roy RR, Edgerton VR (2001) Role of motor unit structure in defining function. Muscle Nerve 24:848–866

Muhlendyck H (1978) The size of motor units in reference to eye-muscle fibers of different innervation. In: Kommerell G (ed) Disorders of ocular motility. Bergmann, Munich, pp 17–26

Nelson JS, Goldberg SJ, McClung JR (1986) Motoneuron electrophysiological and muscle contractile properties of superior oblique motor units in cat. J Neurophysiol 55:715–726

Optican LM, Robinson DA (1980) Cerebellar-dependent adaptive control of primate saccadic system. J Neurophysiol 44:1058–1076

Peachey L (1971) The structure of the extraocular muscle fibers of mammals. In: Bach-y-Rita P (ed) The control of eye movements. Academic Press, New York, pp 47–65

Scudder CA, McGee DM (2003) Adaptive modification of saccade size produces correlated changes in the discharges of fastigial nucleus neurons. J Neurophysiol 90:1011–1026

Scudder CA, Kaneko CRS, Fuchs AL (2002) The brainstem burst generator for saccadic eye movement. A modern synthesis. Exp Brain Res 142:439–462

Shall MS, Goldberg SJ (1992) Extraocular motor units: type classification and motoneuron stimulation frequency-muscle unit force relationships. Brain Res 587:291–300

Shall MS, Goldberg SJ (1995) Lateral rectus EMG and contractile responses elicited by cat abducens motoneurons. Muscle Nerve 18:948–955

Shall MS, Dimitrova DM, Goldberg SJ (2003) Extraocular motor unit and whole muscle contractile properties in the squirrel monkey: summation of forces and fiber morphology. Exp Brain Res 151:338–345

Sylvestre PA, Cullen KE (1999) Quantitative analysis of abducens neuron discharge dynamics during saccadic and slow eye movements. J Neurophysiol 82:2612–2632

Spencer RF, Porter JD (1988) Structural organization of the extraocular muscles. In: Büttner-Ennever JA (ed) Neuroanatomy of the oculomotor system. Elsevier, Amsterdam, pp 33–79

Waldeck RF, Murphy EH, Pinter MJ (1995) Properties of motor units and self-reinnervation of the cat superior oblique muscle. J Neurophysiol 74:2309–2318

Wieczorek DF, Periasamy M, Butler-Browne GS, Whalen RG, Nadal-Ginard B (1985) Co-expression of multiple myosin heavy chain genes, in addition to a tissue-specific one, in extraocular musculature. J Cell Biol 101:618–629